IAP 2006: Report for 1.978

February 3, 2006

Yujie Wei

1 Problem 1

(1.a) The atomic coordinates for the crystallographic orientation of [100] [010] [001] are listed below, in unit of a, for $a = 3.615\mathring{A} = 3.615 \times 10^{-10} m$, being the lattice constant:

(0,0,0)	(1, 0, 0)	(1, 1, 0)	(0, 1, 0)
(0,0,1)	(1, 0, 1)	(1, 1, 1)	(0, 1, 1)
(0.5,0,0.5)	(1, 0.5, 0.5)	(0.5, 1, 0.5)	(0, 0.5, 0.5)
(0.5,0.5,0)	(0.5, 0.5, 1)		

Table 1: Atomic coordinates for the unit cell shown in Fig. 1a, with a crystallographic orientation of [100] [010] [001]

(1.b) The atomic coordinates for the crystallographic orientation of ([110] [$\bar{1}$10] [001]) are listed below, in unit of a:

(0,0,0)	(0.707, 0, 0)	(0.707, 0.707, 0)	(0, 0.707, 0)
(0,0,1)	(0.707, 0, 1)	(0.707, 0.707, 1)	(0, 0.707, 1)
(0.5,0.5,0.5)			

Table 2: Atomic coordinates for the unit cell shown in Fig. 1b, with a crystallographic orientation of ([110] [$\bar{1}$10] [001]).

(2) As shown in Fig. 1a, there are four atoms in this unit cell occupying a volume of a^3. The atomic volume Ω_0 is

$$\Omega_0 = \frac{a^3}{4} = 1.1810 \times 10^{-29}\ m^3 \tag{1}$$

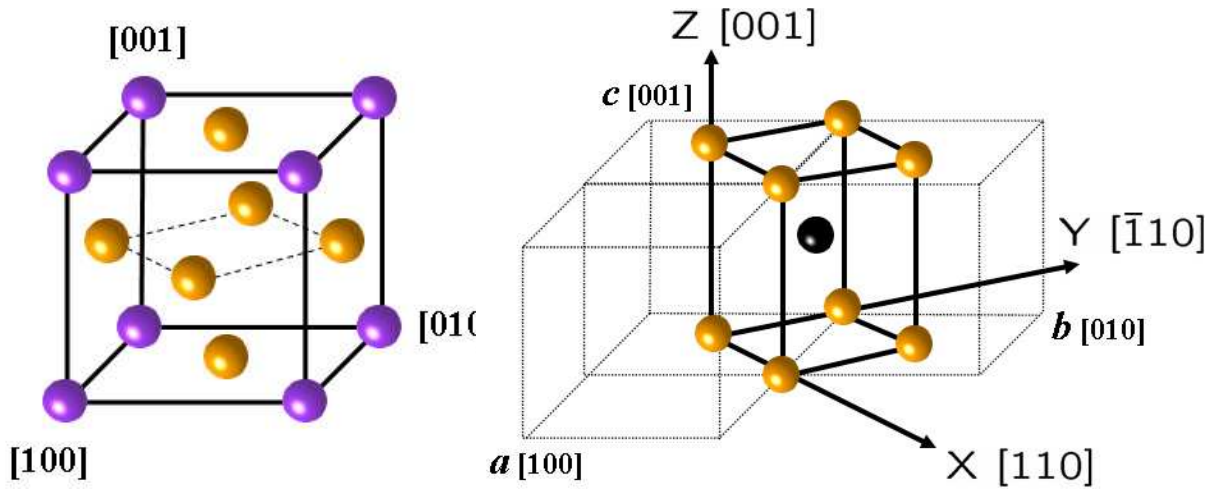

(a) (b)

Figure 1: (a) Atomic coordinates and the unit cell for fcc copper with [100] [010] [001] orientation. (b) Atomic coordinates and the unit cell for fcc copper with [110] [$\bar{1}$10] [001] orientation.

For each copper atom with mass of $m_0 = 63.546amu = 63.546 \times 1.660538 \times 10^{-27}kg$, the density ρ of copper is

$$\rho = \frac{m_0}{\Omega_0} = 8.9345 \times 10^3 \ kg/m^3 \tag{2}$$

2 Problem 2

Following the methodology of Daw and Baskes (1984), the total energy per atom, for a pair potential and nearest neighbor interactions, is

$$E_{tot} = \frac{1}{2}\sum_{i,j}^{12} \phi(R_{ij}) \tag{3}$$

with R_{ij} being the distance between ith atom and jth atom and

$$\phi(r) = 4\varepsilon\left(\left[\frac{\sigma}{r}\right]^{12} - \left[\frac{\sigma}{r}\right]^{6}\right). \tag{4}$$

The first and second derivative of ϕ with respect to r are

$$\phi' = \frac{24\varepsilon}{\sigma}\left(\left[\frac{\sigma}{r}\right]^{7} - 2\left[\frac{\sigma}{r}\right]^{13}\right) \tag{5}$$

$$\phi'' = \frac{24\varepsilon}{\sigma^2}\left(26\left[\frac{\sigma}{r}\right]^{14} - 7\left[\frac{\sigma}{r}\right]^{8}\right) \tag{6}$$

Let one atom sitting at O with coordinate (0,0,0), as shown in Fig. 2. The distances between this atom to its nearest neighbors are a^m, which is equal to $a/\sqrt{2}$. The coordinates of all the nearest neighbors, in unit of a, are: Hence we have

(0.5, 0.5, 0)	(0.5, 0, 0.5)	(0, 0.5, 0.5)	(0, 0.5, -0.5)	(0.5, 0, -0.5)	(0, -0.5, 0.5)
(0, -0.5, -0.5)	(0.5, -0.5, 0)	(-0.5, 0.5, 0)	(-0.5,0, 0.5)	(-0.5, 0, -0.5)	(-0.5, -0.5,0)

Table 3: Atomic coordinates (in unit of a) for all twelve nearest neighbors for the atom sitting at (0,0,0) for fcc copper.

$$A_{ij} = \begin{cases} \frac{a^2}{a^m}\phi'|_{a^m} & \text{if } i = j \\ 0 & \text{otherwise.} \end{cases} \tag{7}$$

and

$$B_{ijkl} = \begin{cases} \frac{a^4}{4(a^m)^2}(\phi'' - \phi'/a^m)|_{a^m} & \text{if } i = j = k = l \\ \frac{a^4}{8(a^m)^2}(\phi'' - \phi'/a^m)|_{a^m} & \text{if } i = j, k = l, i \neq k \\ 0 & \text{otherwise.} \end{cases} \tag{8}$$

(1) The elastic constants, using Equ. 10a-10c in Daw and Baskes (1984) and eliminating those terms associated with embedding energy, are

$$C_{11} = C_{22} = C_{33} = B_{11}/\Omega_0 \tag{9}$$

$$C_{12} = C_{23} = C_{31} = B_{12}/\Omega_0 \tag{10}$$

$$C_{44} = C_{55} = C_{66} = B_{12}/\Omega_0 \tag{11}$$

$$\tag{12}$$

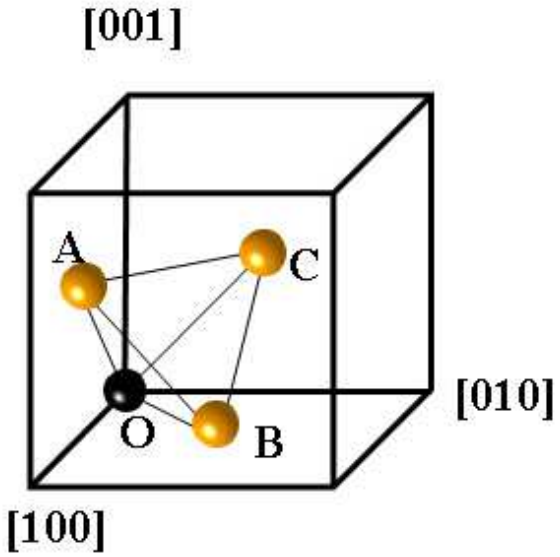

Figure 2: Nearest neighbors (golden atoms) of the atom sitting at O (black atom) in one unit cell.

(2) Equilibrium condition requires $A_{ij} = 0$, hence we have

$$\sigma = \frac{a^m}{\sqrt[6]{2}} = \frac{a}{\sqrt{2} \quad \sqrt[6]{2}}. \tag{13}$$

(3) The potential minimizes at $\phi' = 0$. Hence we could obtain the minimized location $r_0 = \sigma \quad \sqrt[6]{2}$ with $\phi_{min} = \varepsilon$.

(4) Assume isotropic material behavior and we have the following relationships between the elastic constants and the Lamé coefficients:

$$C_{ijkl} = \lambda\delta_{ij}\delta_{kl} + \mu(\delta_{ik}\delta_{jl} + \delta_{il}\delta_{jk}) \tag{14}$$

Therefore,

$$C_{11} = C_{1111} = \lambda + 2\mu \tag{15}$$
$$C_{12} = C_{1122} = \lambda \tag{16}$$

We have, $\lambda = C_{12}$ and $\mu = (C_{11} - C_{12})/2$. With these Lame coefficients λ and μ, we could calculate Young's modulus E, Possion's ratio ν, and bulk modulus K:

$$E = \frac{\mu(3\lambda + 2\mu)}{\lambda + \mu} = \frac{48\varepsilon}{\sigma^3} \tag{17}$$
$$\nu = \frac{\lambda}{2(\lambda + \mu)} = \frac{1}{3} \tag{18}$$
$$K = \frac{3\lambda + 2\mu}{3} = \frac{48\varepsilon}{\sigma^3} \tag{19}$$

(5) There are only two independent elastic constants C_{ijkl} exist for the LJ potential with nearest neighbor interactions. Those are C_{11} and C_{12} or C_{44}.

(6) The Cauchy relation holds for LJ potential. That is $C_{12} = C_{44}$.

(7) σ could be determined using the Equ. 13. Giving $a = 3.615\mathring{\text{A}}$, we have $\sigma = 2.2773\mathring{\text{A}}$. Bulk modulus K for polycrystalline copper is $K = 140\,\text{GPa}$. With

$$K = \frac{48\varepsilon}{\sigma^3}, \tag{20}$$

We can obtain $\varepsilon = 0.215ev$. Compared with those of Cleri et al. (1997), where $\varepsilon = 0.167ev$ and $\sigma = 2.314\mathring{\text{A}}$, the discrepancy from parameters obtained here may arise from the constraint that only the nearest neighbor interaction is allowed in our analytical derivation.

(8) The corresponding results are tabulated in Table 4

Potential	Max. σ (GPa)	Max. ϵ	Unstable ϵ	K (GPa)
EAM (Mishin)	20.7	0.39	0.39	135
LJ (Cleri)	13.0	0.37	0.28	122
LJ (Nearest)	13.1	0.39	0.30	137

Table 4: Simulation on Bulk modulus

Potential	Orientation	Max. σ (GPa)	Max. ϵ	Unstable. ϵ	E (GPa)
EAM	(100)	20	0.23	0.16	165
(Mishin)	(110)	20	0.21	0.21	208
LJ	(100)	16	0.17	0.16	170
(Cleri)	(110)	13.8	0.18	0.13	217
LJ	(100)	17.2	0.21	0.21	190
(Nearest)	(110)	14	0.22	0.20	240

Table 5: Simulation on tensile response

(9) The cohesive energy per atom for the EAM potential is about **-3.544 ev**.

(10) For the harmonic potential in the form of

$$\phi(r) = \epsilon_h + \frac{1}{2}k(r - r_0)^2, \tag{21}$$

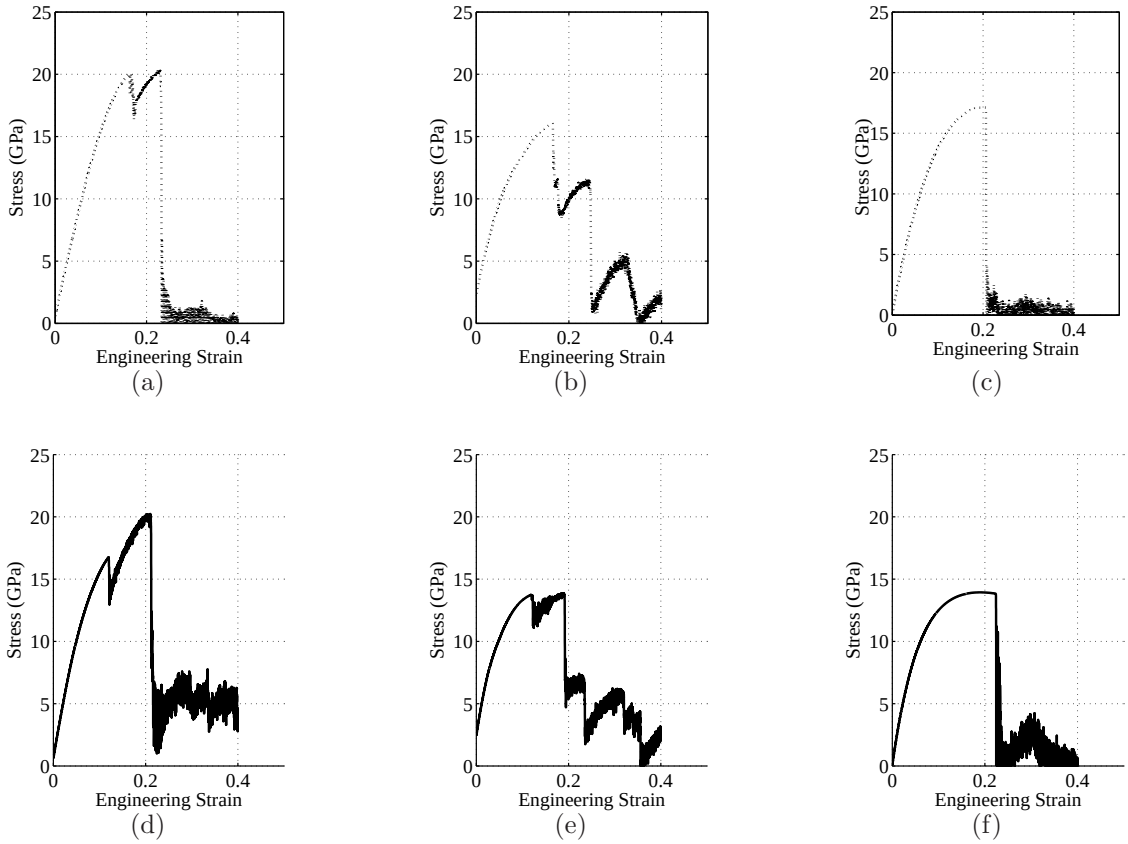

Figure 3: Nominal stress-strain curves from MD simulation on unit cell for fcc copper with [100] [010] [001] orientation. (a) EAM potential. (b) LJ by Cleri et al. (c) LJ, nearest neighbor. (d-e) on unit cell for fcc copper with [110] [$\bar{1}$10] [001] orientation with loading along [110]; (d) EAM potential; (e) LJ by Cleri et al.; (f) LJ, nearest neighbor.

its equilibrium position is r_0. To fit the LJ potential, we have $r_0 = a^m = a/\sqrt{2}$. The minimum energy is $\epsilon_h = \varepsilon$. The stiffness for the harmonic potential at $r = r_0$ is k. For the case of LJ potential, it is

$$\phi''|_{a^m} = \frac{144\varepsilon}{a^2} \tag{22}$$

Hence we have

$$k = \frac{144\varepsilon}{a^2} \tag{23}$$

This potential is only valid in a small region of the equilibrium position. Otherwise, tremendous stress (linear relationship between distance and force) will produce to drag an atom back to its equilibrium. Hence it is impossible to represent large-strain elastic properties. Dislocations are not able to nucleate.

(11) In the case of nearest neighbor interaction, the energy is the same for the two configurations. Therefore, the nearest neighbor interaction misses the energy contribution due to bending in a one-dimensional string of atoms.

3 Problem 3

(1) Please refer to Table 6.

Parameters	Function
coordname	The input file specified the type and coordinates of all atoms
outfiles	Basename for output files
ensemble	Simulation ensemble
startstep	Starting step number
maxsteps	step number at which simulation phase ends
timestep	Size of timestep, in MD units
total_types	Total number of atom types (including virtual types)
ntypes	Number of real atom types
core_potential_file	Tabulated core-core pair potential, EAM
embedding_energy_file	Enbedding Energy Function, EAM
atomic_e-density_file	Electron Density, EAM
box_x	'x' or first vector for box
box_y	'y' or first vector for box
box_z	'z' or first vector for box
restrictionvector	Boundary constraint for an atom type
pbc_dirs	Periodic BC or free BC
max_deform_int	intervals for each deformation
deform_shift	Deforming vector
eng_int	intervals for output energy, pressure, stress et al.
checkpt_int	intervals for output snapshots
starttemp	system temperature at beginning
seed	Seed for random number generator

Table 6: Parameters for an input file and their functions

(2) The length unit is **1 Angstrom** (10^{-10} m)

The energy unit is **1 ev** (1.6022×10^{-19} J)

The time scale is **1.018 fs** (1.018×10^{-14} s)

(3) The integration step is $2.5045 \times 10^{-15} s$

(4) The reference temperature, using the fact that KT is in unit of energy, is **1ev/k = 11605K**. Using the fact that σV has a unit of energy, for V being a volume, the reference stress is **1ev/angstrom ^{3} = 160.2 GPa**.

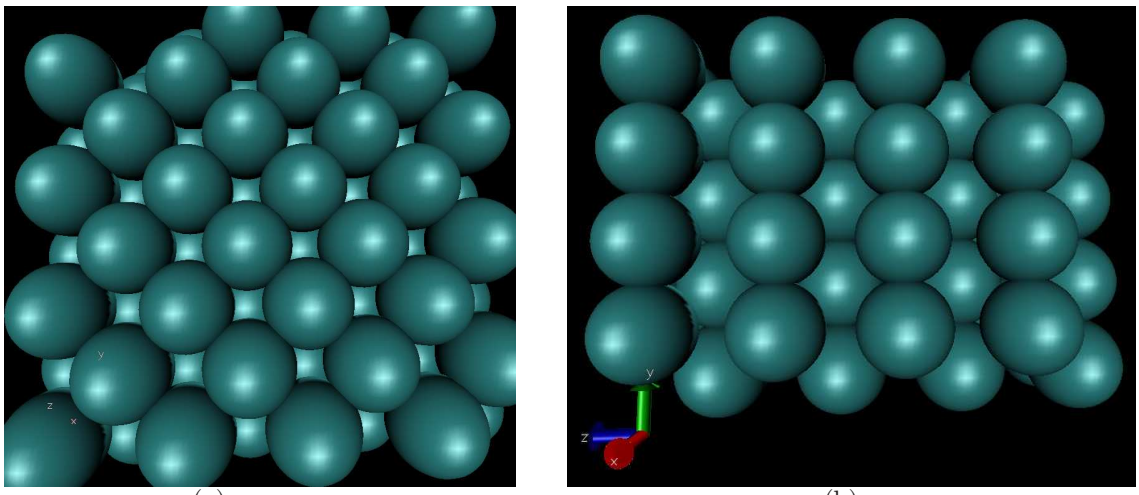

(a) (b)

Figure 4: (a) Perfect crystal with [100] [010] [001] orientation. (b) [110] [$\bar{1}$10] [001] orientation.

(5) Visulization: shown in Fig. 4

(6-7) The structure is generated using fcc_110-crack.c. In order to obtain a crack surface with normal in [001] direction, a structure with about 128 $\mathring{A}$ in x, about 256 $\mathring{A}$ in y, and 7 $\mathring{A}$ in z is constructed. Top and bottom atoms in x direction will be constrained to Mode I crack.

(8) The potential energy versus iteration steps for the cracked structure is shown in Fig. 5. A minimum of about 5000 iteration steps are needed to achieve convergence.

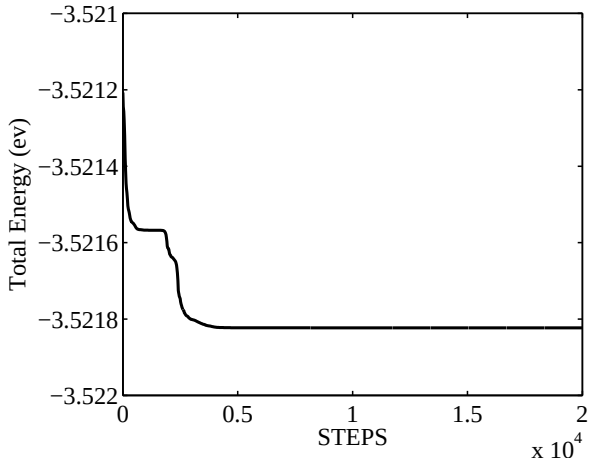

Figure 5: Potential energy per atom of the system versus iteration steps for the energy minimization of the cracked structure.

(9) The cohesive energy for a copper atom at equilibrium is **-3.54 ev**. Atoms in dislocation cores or surfaces usually have higher energy than the critical cohesive energy.

Therefore, to distinguish atoms in dislocation cores, surfaces etc. from perfectly bonded atoms, we need to filter out these atoms with energy high than **-3.54 ev**. A critical potential about -3.4ev might be a good choice to show surface.

(10-11) A start temperature of 100K is chosen to fulfil the requirement. In the IMD system, a value of 100/11605 =0.0086 (11605K corresponds to the temperature of 1ev/k). The temperature versus iteration steps for the cracked structure is shown in Fig. 6. The stable temperature is about 50K. It takes about 5 ps for the system to equilibrate.

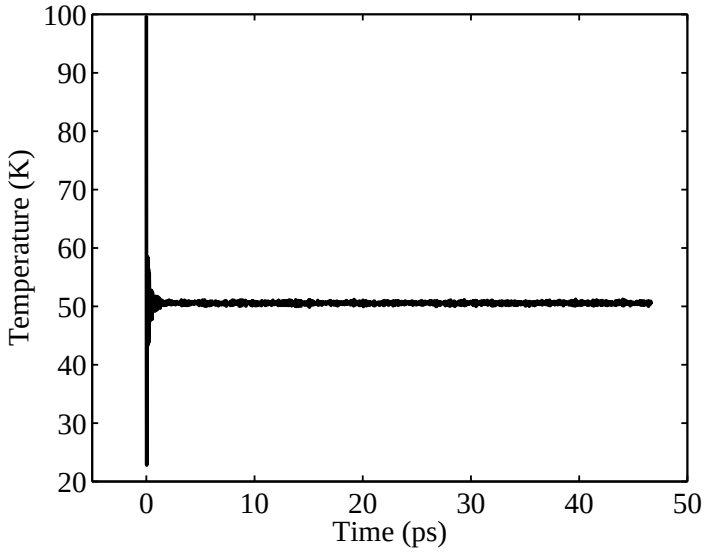

Figure 6: NVE calculation for the temperature (K) evolution as time (ps) for the cracked structure.

(12) The velocity v and strain rate $\dot{\epsilon}$ in boundary atoms are

$$v = \frac{0.05 \times 10^{-10}}{0.25 \times 20 \times 1.018 \times 10^{-14}} \approx 100 m/s \tag{24}$$

$$\dot{\epsilon} = \frac{v}{L} = \frac{0.05}{0.25 \times 20 \times 1.018 \times 10^{-14} \times 122} \approx 8 \times 10^{9}/s \tag{25}$$

(13) Stress-strain curve for the simulation on crack propagation is shown in Fig. 7. The corresponding stiffness is about 73.4 GPa. Due to the geometry, the cracked structure is easier to induce dislocation emission. Hence the instable stress and strain are much smaller than those of perfect crystal. The propagation of a crack will result in a gradually decrease of stress.

(14) As shown in Fig. 8, the crack propagates as dislocations emitted from crack tip and result in a blunt crack. The stress will reduce gradually as the crack extends.

(15) The critical strain for the initiation of dislocation occurs at 3% strain approximately.

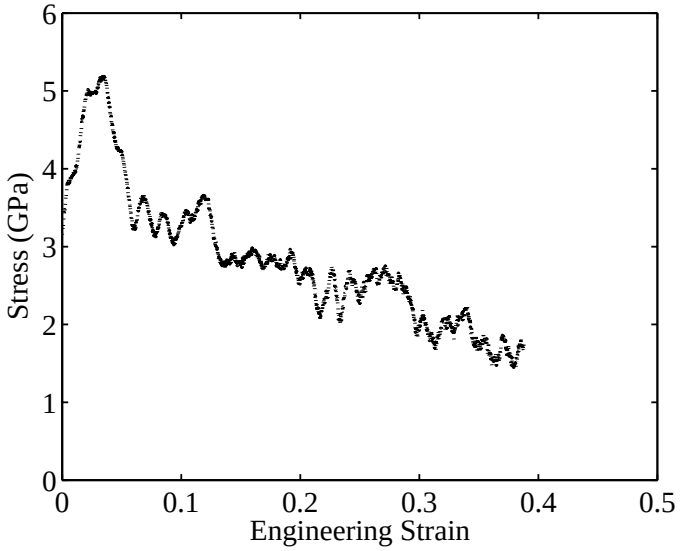

Figure 7: Stress-strain curves for the mode I cracking propagation simulation.

(16) Increase the loading rate will decrease the critical strain for failure.

(17) Several snapshots before and after the onset of crack propagation are shown in Fig. 9.

(18)

$$\xi_{cr} = \frac{4E\gamma}{\sigma_{th}^2(1-\nu^2)} \tag{26}$$

$$= \frac{4 \times 100 \times 10^9 \times 1.5}{10^{20}\ (1-0.3^2)} \tag{27}$$

$$\approx 7 \text{ nm} \tag{28}$$

Flow-tolerance mechanism wouldn't play an important role in copper since at strength much lower than that of the threshold, dislocations will be active. Deformation could be accommodated by dislocation movement, instead of crack propagation. The flaw-tolerance length scale may be of significance in brittle materials, like glass, ceramics et al.

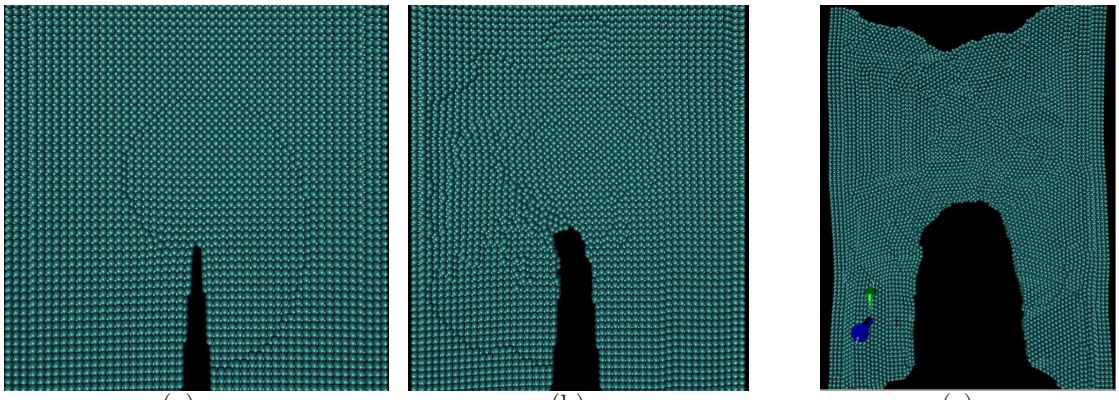

(a) (b) (c)

Figure 8: The mode I cracking propagation simulation. (a) snapshot of atoms at the very beginning (b) snapshot of atoms at the middle of loading, where dislocations emitted from crack tip and free surface are observable. (c) snapshot of simulation when crack propagates two thirds of the sample.

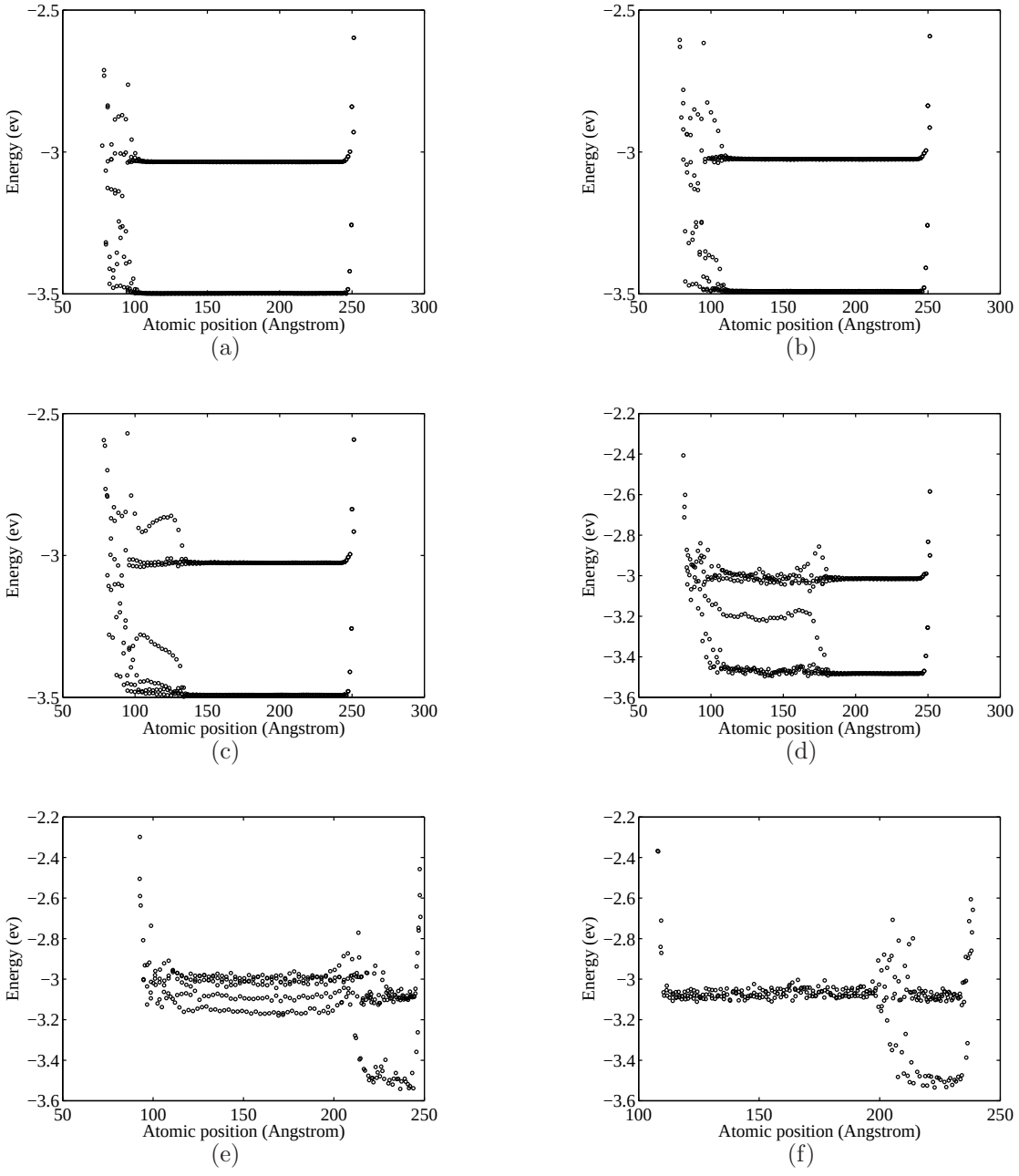

Figure 9: The mode I cracking propagation simulation, energy of the middle layer atoms. (a) before the onset of fracture, at 1% strain. (b) At 2% strain. (c) At 3% strain, where a dislocation is emitted from crack tip. (d) At 4% strain; (e) At 10% strain; and (f) at 20% strain

4 Problem 4

(1) A nanowire with dimension of (25.56Å, 25.56Å, 180.75Å) is constructed with corresponding crystallographic orientation of (110, $1\bar{1}0$, 001). A topside view of the nanowire is shown in Fig. 10

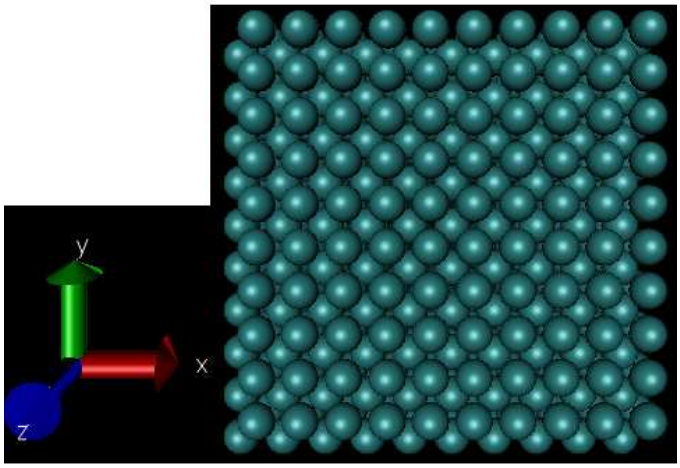

Figure 10: A top side view of the nanowire.

(2) The energy of the structure is minimized (GLOK). The systems evolves to equilibrium very quickly, in less than 700 iteration steps. Energy versus steps is plotted in Fig. 11.

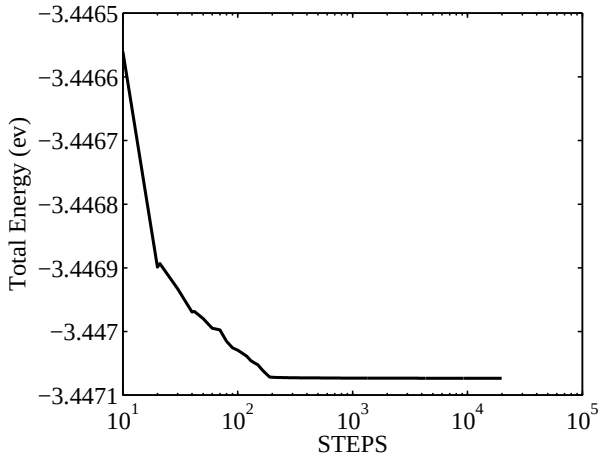

Figure 11: Energy minimization (GLOK) for the nanowire.

(3) Using a displacement rate of 0.1 Å (-0.05 for the bottom boundary and 0.05 for the top boundary) in every 20 steps, the nanowire is stretched with periodic boundary condition in x and y.

(4) The velocity v and strain rate $\dot{\epsilon}$ in boundary atoms are

$$v = \frac{0.1 \times 10^{-10}}{0.25 \times 20 \times 1.018 \times 10^{-14}} \approx 200m/s \tag{29}$$

$$\dot{\epsilon} = \frac{v}{L} = \frac{0.1}{0.25 \times 20 \times 1.018 \times 10^{-14} \times 250} \approx 8 \times 10^{9}/s \tag{30}$$

(5) The stress versus strain along the loading axis is plotted in Fig. 12. Compared with the stress-strain curve with the same crystal orientation but having periodic boundary conditions, the peak stress for a nanowire under tension is much lower. Also, the modulus here is about 74 GPa. In the case with periodic boundary condition, it is not a simple tension test. Stress component in the other two direction are quite large. Deformation is hard to localize. In the case of free-boundary condition in nanowire test, materials are allowed to contract in the transverse direction. Defects are easier to initiate in free surfaces. Therefore, it is easier to induce localized necking.

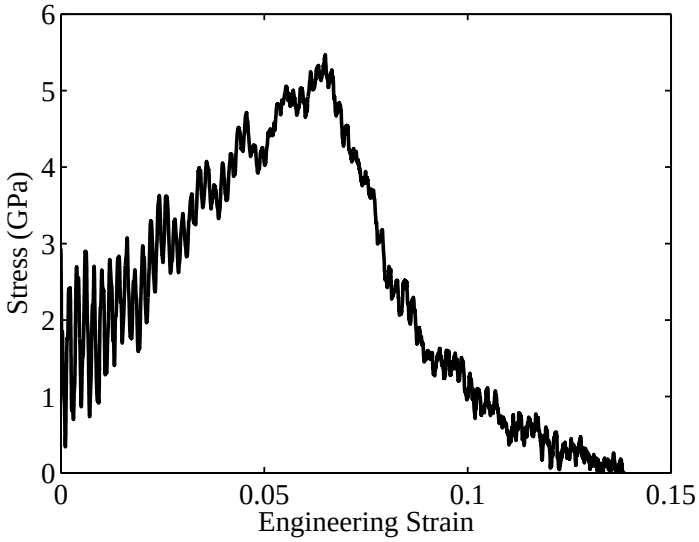

Figure 12: (a) Nominal stress-strain curve for the nanowire subject to uniaxial tension. The oscillation is due to the large increment we applied. I actually used an increment of 0.01 Angstrom each 20 steps, with a increment of 0.125 (system units). Slow boundary velocity is desired to obtain a smooth stress-strain curve

(6) The critical strain is only about 6% at the onset of failure. In macroscopic polycrystalline Cu, an elongation of more than 100% could be achieved. It is mainly because of defects like dislocations in polycrystalline Cu which accommodate the necessary deformation.

(7) In the cracked crystal, deformation along crack tip is accommodated by emission of dislocations from the tip. Due to the geometry we supply, such a process is able to

blunt the sharp crack at the beginning, as seen in Fig. 8a-c. As to the case of the nanowire with orientation of (110, $1\bar{1}0$, 001), the Schmid factor for the four planes and the eight easy-slip systems are all the same $\frac{1}{\sqrt{6}}$. It is more likely to induce necking instead of preferred slip along one slip system.

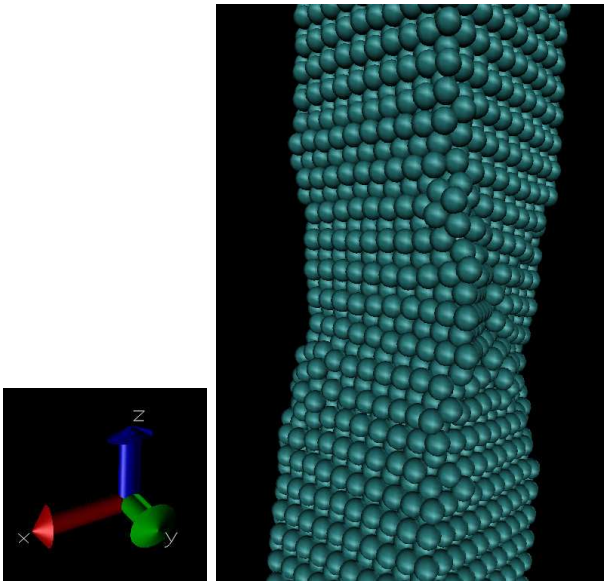

Figure 13: A snapshot from the simulation shows the necking region, high energy atoms $> 3.45ev$ and boundary atoms are removed..

(8) The poisson's ratio ν is estimated by tracking two atoms on the same layer (the same **Z** coordinate) to obtain the contraction of the cross-section. A plot of the total engineering strain versus the lateral strain is shown in Fig. 14. An approximate value

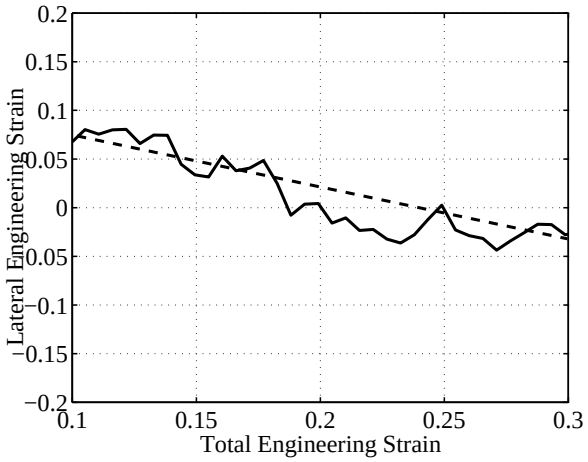

Figure 14: Poisson's ratio estimation based on axial and lateral strains.

of 0.36 is obtained. Experimental Poisson's ratio for polycrystalline Cu is about 0.34.

References

Daw, M.S. and Baskes, M.I., Embedded-atom method: Derivation and application to impurities, surfaces, and other defects in metals, Phys. Rev. B., 1984;29:6443-6453.

Simmons, G. and Wang, H., *Single Crystal Elastic Constants and Calculated Aggregate Properties*, The M.I.T. Press, Cambridge, 1971.

Cleri, F. and Yip, S. and Wolf, D. and Phillpot, S.R., Atomic-Scale mechanism of crack-tip plasticity: dislocation nucleation and crack-tip shielding, Physical Review B 1997:1309-12.